Synthesis and Characterization of Silica-Encapsulated Iron Oxide Nanoparticles

Yimeng Du[1], Li Li[1], C. W. Leung[2], P. T. Lai[1], and Philip W. T. Pong[1]

[1]Department of Electrical and Electronic Engineering, The University of Hong Kong, Hong Kong
[2]Department of Applied Physics, The Hong Kong Polytechnic University, Hung Hom, Hong Kong

The properties of magnetic core-shell nanoparticles greatly depend on their core sizes and shell materials. Silica shell can prevent the magnetic nanoparticles from corrosion and agglomeration. In addition, the hydrolyzed silica can provide silanol groups to facilitate surface biofunctionalization. In this paper, superparamagnetic Fe_3O_4 nanoparticles coated with SiO_2 shell were prepared by a one-pot water-in-oil microemulsion method. Transmission electron microscopy (TEM), scanning electron microscopy (SEM), and vibrating sample magnetometry (VSM) were utilized to characterize the morphology and magnetic properties of the synthesized nanoparticles. The results indicated that by tuning the water/surfactant molar ratio (Wo) of the microemulsion system, core size of the resulting Fe_3O_4 nanoparticles can be altered. The size-controllable silica-encapsulated Fe_3O_4 superparamagnetic nanoparticles have great potential to be applied as multifunctional tracer materials for magnetic particle imaging (MPI).

Index Terms—Core-shell nanoparticles, iron oxide nanoparticles, magnetic particle imaging (MPI), microemulsion.

I. INTRODUCTION

IN recent years, iron oxide nanoparticles (IONPs) have attracted extensive attention because of their low toxicity, biocompatibility, and environmental friendliness [1], [2]. Typically, IONPs smaller than a critical diameter are superparamagnetic nanoparticles that possess a large constant magnetic moment but negligible remanence and coercivity [3]. Taking advantage of the characteristic nonlinear response of superparamagnetic IONPs to an oscillating magnetic field, a novel tomographic imaging modality named magnetic particle imaging (MPI) was developed in 2005 [4]–[6]. Superparamagnetic IONPs applied as the contrast agent for MPI are called tracer materials, and the oscillating magnetic field is called a modulation field. In order to enhance MPI performance, relaxation of the tracer material should be optimized according to the modulation field frequency [7]. Simulation studies have indicated that nanoparticle size and size distribution govern nanoparticle relaxation [8]. As a result, it is worthwhile to explore a synthetic route of monodisperse IONPs with controllable size for application as MPI tracer materials.

Water-in-oil microemulsion is one of the powerful synthesis technologies producing IONPs with a high degree of crystallinity [9]. In a water-in-oil microemulsion system, reverse micelles containing aqueous solution are dispersed in the hydrocarbon solvent [3] as nanoreactors for aqueous reactions. It has been documented that the size of the reverse micelle greatly depends on the value of water/surfactant molar ratio (Wo) [10]. As a result, the sizes of the resulting IONPs can be easily controlled by tuning the values of Wo. Moreover, the microemulsion technology can be carried out at room temperature and applied in mass production [11]. Thus, this facile water-in-oil microemulsion technology is a promising

candidate for the synthesis of different sizes of IONPs as MPI tracer materials.

IONPs tend to aggregate in aqueous solutions due to their small sizes and hydrophobicity [3], [12], [13]. In addition, the magnetic property of IONPs must be preserved in the biological environment from degradation when used as MPI tracer materials [5]. Consequently, surface modifications are required to avoid aggregation and facilitate the performance of IONPs in MPI applications. Core-shell structure was proposed to this end [14]. Amorphous silica possesses fascinating chemical stability and hence is one of the popular shell materials. The nanothin silica shell leaves the morphology and magnetic property of the IONPs intact while preventing the magnetic cores from flocculation, agglomeration, and corroding [13]. The silica shell can be further modified to attach optical, physical, chemical, or biomedical functional groups for different purposes such as drug delivery, bioseparation, and diagnostic analysis [1], [3], [10], [15], [16]. Such silica-encapsulated IONPs show promise as MPI tracer materials for multifunctional biomedical modalities which may combine therapeutic and diagnostic strategies.

The purpose of this work is to develop a promising candidate method for preparing size-controllable MPI tracer materials based on the one-pot water-in-oil microemulsion technology [10]. Here, microemulsion technology was used to synthesize silica-encapsulated IONPs at room temperature. In addition, the effect of Wo on the size of the IONP cores was investigated. The morphology and magnetic property of the synthesized silica-encapsulated IONPs were characterized.

II. EXPERIMENTAL SECTION

1) Chemicals: Iron (II) chloride tetrahydrate (99+%), tetraethyl orthosilicate (TEOS) (98%), hexadecyltrimethylammonium bromide (CTAB) (99+%), ammonium hydroxide (28–30 wt% in water), toluene (99.5%), and ethanol (99.8%) were purchased from Acros Organics. Iron (III) chloride hexahydrate (98+%) was purchased from Sigma-Aldrich. All of the chemicals were used as-received without further treatment.

2) Synthesis Procedure: A previously reported microemulsion system was used in this study [10]. The water-in-oil mi-

TABLE I
THREE PROTOCOLS FOR SYNTHESIS OF IONPS

Wo	$FeCl_2 \cdot 4H_2O$	$FeCl_3 \cdot 6H_2O$	DI water
26	0.0685g	0.1864g	1.8879g
40	0.1028g	0.2796g	2.8319g
80	0.2056g	0.5592g	5.6638g

croemulsion was formed using aqueous $FeCl_2/FeCl_3$ solution and excess toluene with the help of CTAB as a surfactant. Wo is the molar ratio of deionized (DI) water to CTAB. In this study, Wo was adjusted by changing the amount of aqueous solution while all the other experimental conditions were fixed. As shown in Table I, three protocols (Wo = 26, 40, and 80) were used to produce three groups of IONPs by following the procedure of *synthesis of IONPs*. In order to synthesize the core-shell nanoparticles, a second step (*formation of silica shell*) was performed after the first step (*synthesis of IONPs*) in a one-pot manner. The two synthesis steps are described in detail as follows.

Synthesis of IONPs: First of all, 1.4578g of CTAB was dispersed into 30 g of predried toluene in a round bottom flask under vigorous stirring. Afterwards, according to the three protocols shown in Table I, $FeCl_2 \cdot 4H_2O$ and $FeCl_3 \cdot 6H_2O$ were dissolved in DI water, and this $FeCl_2/FeCl_3$ solution was slowly dropped into the toluene suspension under a nitrogen atmosphere. After that, the system was stirred continuously for 4h. Excess ammonia solution, in this case 1.3 ml, was then slowly added to the microemulsion system under a nitrogen atmosphere. The suspension immediately turned black indicating the formation of Fe_3O_4 nanoparticles. The chemical reaction for this procedure is as follows:

$$FeCl_2 + 2FeCl_3 + 8NH_3 \cdot H_2O \rightarrow Fe_3O_4 + 8NH_4Cl + 4H_2O$$
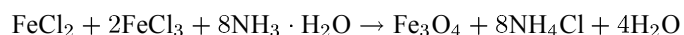
Formation of silica shell: Two hours after adding ammonia, 1.3870g of TEOS was slowly added into the flask under a nitrogen atmosphere. The system was then stirred continuously for 5 days to allow the formation of silica shell. At the end of the experiment, ethanol was added to the black microemulsion mixture. The black product was separated by an external magnet and the supernatant was discarded. After washing by ethanol several times, the black precipitate was refluxed in ethanol for 10 h, and then washed several times by DI water. Silica-encapsulated IONPs were prepared for the Wo = 40 protocol in this work.

3) Characterization: Transmission electron microscopy (TEM) images and electron diffraction patterns were obtained using an FEI Tecnai G2 20 S-TWIN Scanning Transmission Electron Microscope. Energy dispersive X-ray spectroscopy (EDS) was performed using a Hitachi S-3400N Variable Pressure Scanning Electron Microscope (SEM). The magnetic property studies were carried out at room temperature using a Lakeshore 7407 vibrating sample magnetometer (VSM).

III. RESULTS AND DISCUSSION

Silica-encapsulated IONPs were successfully synthesized by this water-in-oil microemulsion technology. The shape and size
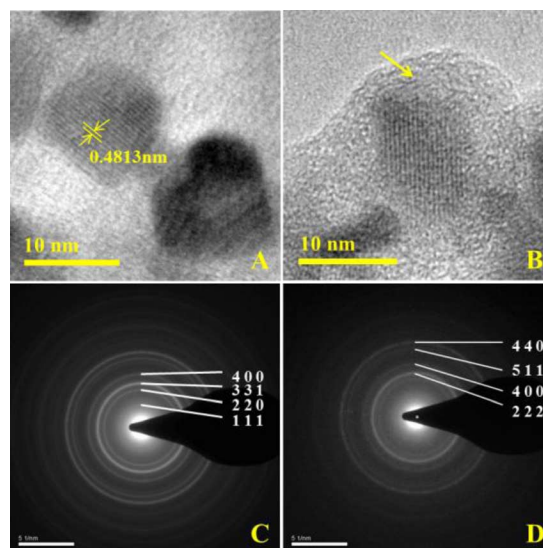

Fig. 1. TEM images of IONPs (A) without and (B) with shell prepared by the protocol of Wo = 40. (A) Lattice fringes were clearly shown in image, and the distance between two adjacent lattice fringes is measured. Amorphous shell (arrow) and crystalline core shown in image (B) indicate the core-shell structure. Electron diffraction patterns of the IONPs (C) without and (D) with shell both reveal Fe_3O_4 crystalline diffraction pattern.
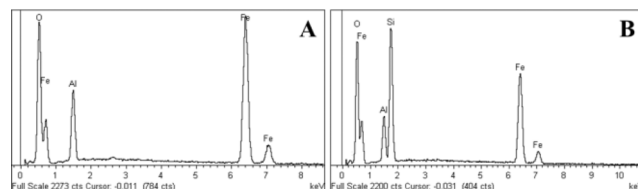

Fig. 2. EDS spectra for IONPs (A) without and (B) with shell that synthesized by the protocol of Wo = 40. Al peaks in the spectra come from the aluminium foil used as the holder for the SEM study.

of the IONP cores without shell [Fig. 1(A)] are similar to those in the core-shell structure [Fig. 1(B)]. The core-shell structure, composed of nanothin amorphous shell and crystalline core, is clearly shown on the TEM image [Fig. 1(B)]. The lattice fringes shown in Fig. 1(A) suggest the high crystallinity of the IONPs. The distance between two adjacent lattice fringes (0.4813 nm) agrees well with the d111 spacing (0.48479 nm) of Fe_3O_4 (JCPDS 86-1362). In addition, the electron diffraction was performed by using TEM for the IONPs without silica shell [Fig. 1(C)] and silica-encapsulated IONPs [Fig. 1(D)]. The two diffraction patterns both present characteristic rings of Fe_3O_4. It is clearly demonstrated that the IONPs are Fe_3O_4 nanoparticles in both cases. The EDS spectra for IONPs (Wo = 40) without [Fig. 2(A)] and with [Fig. 2(B)] silica shell were obtained using SEM. It is obvious that the shell-encapsulated IONPs are composed of Si, Fe, and O, whereas the Si peak disappears in the spectrum of the IONPs without shell. Moreover, the atomic ratios for the shell-encapsulated IONPs are Fe : O : Si = 16.55 : 56.35 : 13.80. This suggests that the compositions of the core-shell nanoparticles are SiO_2 shell and Fe_3O_4 cores, which indicates the silica-encapsulated Fe_3O_4 ($Fe_3O_4@SiO_2$) nanoparticles were synthesized as expected.

In water-in-oil microemulsion process, the size of the aqueous microemulsion droplet directly depends on the value
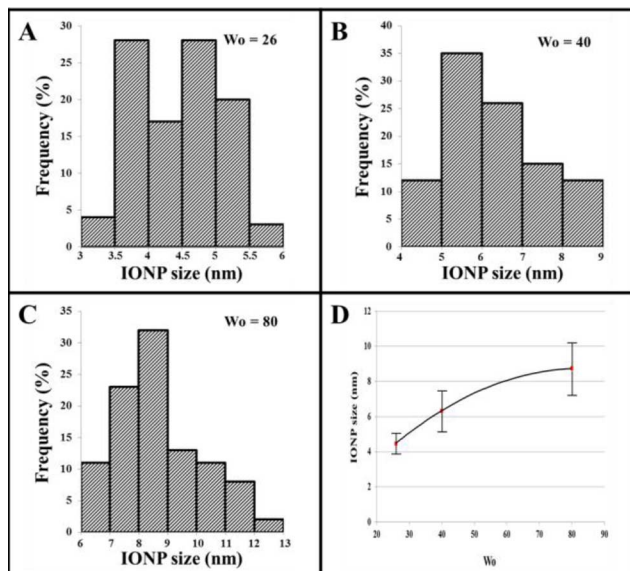
Fig. 3. Size distribution histograms for IONPs without silica shell synthesized by protocol of Wo = (A) 26, (B) 40, and (C) 80, respectively. (D) Relation between the average sizes of IONPs and Wo. Whiskers stand for the standard deviation, and the trendline is added to guide eyes.

Fig. 4. (A) Hysteresis loops of Fe_3O_4 nanoparticles without silica shell. Inset shows the relation between Wo and Ms. Trendline is added to guide eyes. (B) Hysteresis loops for silica-encapsulated Fe_3O_4 nanoparticles ($Fe_3O_4@SiO_2$) and the Fe_3O_4 nanoparticles without silica shell that were both produced with Wo = 40.

of Wo, and it is reasonable to presume that the size of the IONPs directly relates to the Wo value. The IONP size distribution histograms for the protocol of Wo = 26, 40, and 80 are shown in Fig. 3(A), (B), and (C), respectively. The sizes are 4.4 ± 0.59 nm (Wo = 26), 6.3 ± 1.17 nm (Wo = 40), and 8.7 ± 1.49 nm (Wo = 80), respectively. The relation between the average sizes and the Wo values is plotted in Fig. 3(D). In general, the size of the Fe_3O_4 nanoparticles increases with the value of Wo, which coincides with the previous report [10]. This water-in-oil procedure provides a convenient way for preparing different sizes of Fe_3O_4 nanoparticles and by simply adding the second synthesis step (*formation of silica shell*) silica-encapsulated Fe_3O_4 nanoparticles of different sizes could be prepared as well.

The magnetic properties of the resultant nanoparticles were investigated by VSM at room temperature. The hysteresis loops for the Fe_3O_4 nanoparticles without silica shell and the silica-encapsulated Fe_3O_4 nanoparticles are shown in Fig. 4. It is evident that all of the samples show no magnetic hysteresis. Their magnetization and demagnetization curves superimpose with each other and pass through the origin. This implies the superparamagnetic nature which is an important property for MPI tracer material. In addition, Fig. 4(A) shows that the magnitude of the saturation magnetization (Ms) increases with Wo owing to the increase of the Fe_3O_4 nanoparticle size. The trend between Ms and Wo is shown in the inset of Fig. 4(A). Fig. 4(B) shows the hysteresis loops of the silica-encapsulated Fe_3O_4 nanoparticles ($Fe_3O_4@SiO_2$) and the Fe_3O_4 nanoparticles without silica shell. Both were produced with Wo = 40. Although the sizes of the Fe_3O_4 cores in the core-shell structure are similar to the Fe_3O_4 nanoparticles [Fig. 1(A) and (B)], the silica-encapsulated Fe_3O_4 nanoparticles ($Fe_3O_4@SiO_2$) exhibit lower Ms. This can be explained by the fact that the silica shell is nonferromagnetic
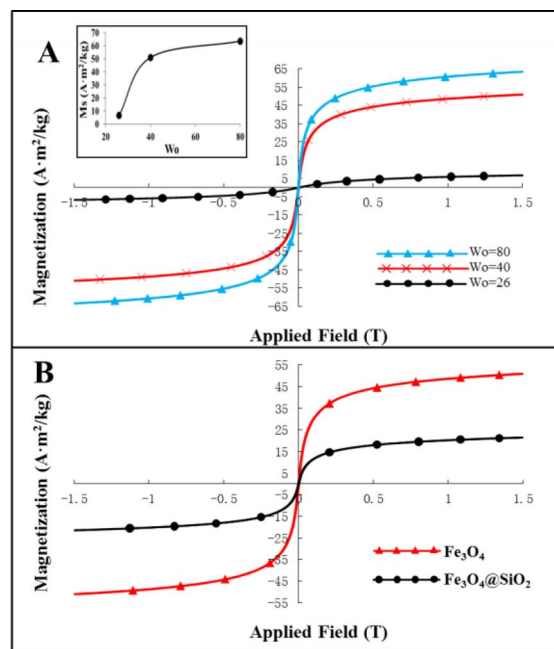
and the Ms only arises from the Fe_3O_4 cores of the silica-encapsulated IONPs [17]. Since the weight percentage of Fe_3O_4 in the silica-encapsulated Fe_3O_4 nanoparticles is lower, its Ms is lower. However, these silica-encapsulated Fe_3O_4 nanoparticles, due to their larger size of Fe_3O_4 cores, still have higher Ms than the Fe_3O_4 nanoparticles without shell produced by Wo = 26. Using this water-in-oil microemulsion method, the size and magnetic property of the promising MPI tracer material, silica-encapsulated Fe_3O_4 nanoparticles, could both be controlled by varying Wo.

IV. CONCLUSION

In this paper, core-shell structured IONPs have been synthesized by using a one-pot water-in-oil (water/CTAB/toluene) microemulsion technology. The core is high-crystallinity Fe_3O_4 and the shell is amorphous silica. These silica-encapsulated Fe_3O_4 nanoparticles are superparamagnetic, and thus they might be a suitable tracer material for MPI. Wo is the key parameter to control the size and magnetic property of the Fe_3O_4 nanoparticles. In conclusion, this water-in-oil microemulsion technology has the potential to produce MPI tracer materials of various sizes and magnetic properties for different MPI applications. Further studies will be carried out to strengthen the control on the size distribution and the shape of the synthesized nanoparticles. Multifunctional MPI materials based on the silica-encapsulated Fe_3O_4 nanoparticles will also be studied.

REFERENCES

[1] M. Bu and W. Ma, "Study on core-shell-shell structured nanoparticles with magnetic and luminescent features: Construction, characterization and oxygen-sensing behavior," *J. Lumin.*, vol. 141, pp. 80–86, Sep. 2013.

[2] M. Mahmoudi, S. Sant, B. Wang, S. Laurent, and T. Sen, "Superparamagnetic iron oxide nanoparticles (SPIONs): Development, surface modification and applications in chemotherapy," *Adv. Drug Deliv. Rev.*, vol. 63, pp. 24–46, Jan.–Feb. 2011.

[3] A. H. Lu, E. L. Salabas, and F. Schuth, "Magnetic nanoparticles: Synthesis, protection, functionalization, and application," in *Angew. Chem. Int. Ed. Engl.*, Feb. 2007, vol. 46, pp. 1222–1244.

[4] B. Gleich and J. Weizenecker, "Tomographic imaging using the nonlinear response of magnetic particles," *Nature*, vol. 435, pp. 1214–1217, Jun. 2005.

[5] A. P. Khandhar, R. M. Ferguson, H. Arami, and K. M. Krishnan, "Monodisperse magnetite nanoparticle tracers for in vivo magnetic particle imaging," *Biomaterials*, vol. 34, pp. 3837–3845, May 2013.

[6] J. Weizenecker, B. Gleich, J. Rahmer, H. Dahnke, and J. Borgert, "Three-dimensional real-time in vivo magnetic particle imaging," *Phys. Med. Biol.*, vol. 54, pp. L1–L10, Mar. 2009.

[7] R. M. Ferguson, K. R. Minard, and K. M. Krishnan, "Optimization of nanoparticle core size for magnetic particle imaging," *J. Magn. Magn. Mater.*, vol. 321, pp. 1548–1551, 2009.

[8] P. C. Fannin, "Investigating magnetic fluids by means of complex susceptibility measurements," *J. Magn. Magn. Mater.*, vol. 258–259, pp. 446–451, Mar. 2003.

[9] C. Okoli *et al.*, "Comparison and functionalization study of microemulsion-prepared magnetic iron oxide nanoparticles," *Langmuir*, vol. 28, pp. 8479–8485, Jun. 2012.

[10] S. C. Tsang, C. H. Yu, X. Gao, and K. Tam, "Silica-encapsulated nanomagnetic particle as a new recoverable biocatalyst carrier," *J. Phys. Chem. B*, vol. 110, pp. 16914–16922, Aug. 2006.

[11] Y. J. Lee *et al.*, "Large-scale synthesis of uniform and crystalline magnetite nanoparticles using reverse micelles as nanoreactors under reflux conditions," *Adv. Funct. Mater.*, vol. 15, pp. 503–509, Dec. 2005.

[12] Z. Liu, G. Yi, H. Zhang, J. Ding, Y. Zhang, and J. Xue, "Monodisperse silica nanoparticles encapsulating upconversion fluorescent and superparamagnetic nanocrystals," *Chem. Commun.*, pp. 694–696, 2008.

[13] G. A. Sotiriou *et al.*, "Hybrid, silica-coated, janus-like plasmonic-magnetic nanoparticles," *Chem. Mater.*, vol. 23, pp. 1985–1992, Apr. 2011.

[14] W. Schartl, "Current directions in core-shell nanoparticle design," *Nanoscale*, vol. 2, pp. 829–843, Jun. 2010.

[15] M. Kokate, K. Garadkar, and A. Gole, "One pot synthesis of magnetite-silica nanocomposites: Applications as tags, entrapment matrix and in water purification," *J. Phys. Chem. A*, vol. 1, pp. 2022–2029, 2013.

[16] Y. Deng, D. Qi, C. Deng, X. Zhang, and D. Zhao, "Superparamagnetic high-magnetization microspheres with an $Fe_3O_4@SiO_2$ core and perpendicularly aligned mesoporous SiO_2 shell for removal of microcystins," *J. Am. Chem. Soc.*, vol. 130, pp. 28–29, Jan. 2008.

[17] G. Zhang, Y. Liao, and I. Baker, "Surface engineering of core/shell iron/iron oxide nanoparticles from microemulsions for hyperthermia," *Mater. Sci. Eng. C. Mater. Biol. Appl.*, vol. 30, pp. 92–97, Jan. 2010.